Journal of Materials Chemistry A

Accepted Manuscript

ROYAL SOCIETY OF CHEMISTRY

www.rsc.org/materialsA

Journal Name

ARTICLE

Impact of Alkyl Side Chains Position on the Photovoltaic Properties of Solution-Processable Organic Molecule Donor Materials

Received 00th January 20xx,
Accepted 00th January 20xx

DOI: 10.1039/x0xx00000x

www.rsc.org/

J. Zhang,[a] X. W. Zhu,[b] C. He,[c] H. J. Bin,[c] L. W. Xue,[c] W. G. Wang,[c] Y. K. Yang,[c] N. Y. Yuan,[a*] J. N. Ding,[a*] Z. X. Wei,[b*] Z. -G. Zhang,[c] and Y. F. Li[c*]

Two new A-D-A structured organic molecules with bithienyl-substituted benzodithiophene (BDT) as core and donor unit, indenedione (ID) as end group and acceptor unit, 3,3''-dihexyl-2,2':5',2''-terthiophene (3T(3-Hex)) or 4,4''-dihexyl-2,2':5',2''-terthiophene (3T(4-Hex)) as π bridge, BDT-3T(3-Hex)-ID and BDT-3T(4-Hex)-ID, were designed and synthesized. The two compounds with the alkyl side chains at different position in the π bridge backbone which are applied in solution-processable organic solar cells (OSCs) as donor material, own the same molecular weight and similar structure, but exhibit different optical and photovoltaic properties. BDT-3T(4-Hex)-ID film shows a broad absorption band from 400 nm to 750 nm with absorption peak about 20 nm red-shifted than that of BDT-3T(3-Hex)-ID in solution, benefitted from the outward alkyl side chain in its structure. The power conversion efficiency (PCE) of the solution-processed OSC based on a blend of BDT-3T(4-Hex)-ID and $PC_{71}BM$ (1.25:1, w/w) reached 6.55% with a J_{sc} of 10.54 mA/cm^2, a V_{oc} of 0.87 V and a *FF* of 71.4%, under the illumination of AM.1.5, 100 mW/cm^2. In comparison, the PCE of the OSC based on BDT-3T(3-Hex)-ID as donor is 1.06% under the same experimental conditions.

Introduction

Bulk heterojunction organic solar cells (OSCs) based on solution-processable organic molecule photovoltaic materials have drawn much attention and research interests in recent years.[1-26] The advantages of solution-processable organic molecule OSCs include easy fabrication, light weight, flexibility, low cost and the definite molecular weight which can avoid the difference from bath to bath in comparison with the polymers. Among the soluble organic photovoltaic molecules, the acceptor-donor-acceptor (A-D-A) structured materials have been the focus of research for their broad absorption in visible region and their lower HOMO levels.[10-26] For example, Chen et al. published a series of A-D-A small molecular donor materials based on oligothiophenes and rhodanine derivatives which have the similar backbones but different conjugation length (DRCN4T-DRCN9T). The OPV devices based on all of the compounds DRCN5T-DRCN9T exhibit good photovoltaic performances with PCEs of over 6%, especially, DRCN5T shows the notable PCE of 10.10%. [20-21]

More and more studies have demonstrated the length of the π bridge, the number, length, branching and position of the side alkyl chains can have significant influence on the optical, crystal, electronic properties and device performance of the photovoltaic materials.[27-37] For example, Prof. Wong' s group published a range of works studying the effect of the various side chain on the photovoltaic properties, the photovoltaic properties of the materials make big difference even a small change from the oxygen atom to sulphur atom in the side chain.[38-44] In previous work, we report four A-D-A molecules based on bithienyl-substituted benzodithiophene (BDT) and indenedione (ID) unit. The highest PCE of the OSCs achieved based on these molecules (D1, D2, DO1, DO2) is 6.75%, which is among the high values in the OSCs based on the solution-processed organic small molecules.[13] In this work, we design and synthesize two new molecules based on BDT as donor unit, ID as acceptor unit, 3,3''-dihexyl-2,2':5',2''-terthiophene (3T(3-Hex)) or 4,4''-dihexyl-2,2':5',2''-terthiophene (3T(4-Hex)) as π bridge, BDT-3T(3-Hex)-ID and BDT-3T(4-Hex)-ID, as shown in Scheme 1. Comparing with D1 which involves bi-thiophene as the π bridge, there is terthiophene with two hexyl side chains as the longer π bridge to extend the π conjugated length in the two new materials. The difference in molecular structure of BDT-3T(3-Hex)-ID and BDT-3T(4-Hex)-ID is just the substituent position of the side chains in the shoulder of the terthiophene. For BDT-3T(3-Hex)-ID, the alkyl side chains concentrated in the center part of the terthiophene backbone to form a inboard configuration, and for BDT-3T(4-Hex)-ID, the chains distributes in the peripheral part of the backbone to

[a] School of Materials Science & Engineering, Jiangsu Collaborative Innovation Center of Photovoltaic Science & Engineering, Changzhou University, Changzhou 213164, Jiangsu, China. *Email: nyyuan@cczu.edu.cn; dingjn_cczu@163.com
[b] National Center for Nanoscience and Technology, Beijing 100190, China. *Email: weizx@nanoctr.cn
[c] Beijing National Laboratory for Molecular Sciences, CAS Key Laboratory of Organic Solids, Institute of Chemistry, Chinese Academy of Sciences, Beijing 100190, China. *E-mail: liyf@iccas.ac.cn

form a outward configuration. It is first to investigate the influence of the side chain position in the π conjugated backbone on OSCs device performance of the corresponding molecular materials. The bulk heterojunction OSCs were obtained by spin-coating the blend solution of the compounds as donor material and $PC_{71}BM$ as acceptor material. The best photovoltaic performance of the OSC devices based on a blend of BDT-3T(4-Hex)-ID and $PC_{71}BM$ (1.25:1, w/w) exhibited a PCE of 6.55% with a short circuit current density (J_{sc}) of 10.54 mA/cm^2, a V_{oc} of 0.87 V and a fill factor (*FF*) of 71.4%, under the illumination of AM.1.5, 100 mW/cm^2. The PCE of 6.55% is comparable with the value of 6.75% for D1.[13] But the PCE of the OSC device based on the blend of BDT-3T(3-Hex)-ID and $PC_{71}BM$ (1:1.5, w/w) is just 1.06%, which confirms that even a tiny change in the position of the side alkyl chains may result in a tremendous impact on photovoltaic device performance.[33]

Experimental details

General

Tris(dibenzylideneacetone)dipalladium [$Pd_2(dba)_3$], tri-tert-butylphosphine tetrafluoroborate [$(CH_3)_3C]_3PHBF_4$, potassium phosphate (K_3PO_4), and 1,3-indanedione were obtained from Acros Organics. Toluene was dried over Na/benzophenone and freshly distilled prior to use. Other chemicals were common commercial level and were used as received.

Experimental

MALDI-TOF spectra were recorded on a Bruker BIFLEX ⍰. Nuclear magnetic resonance (NMR) spectra were taken on a Bruker DMX-400 spectrometer. The thermogravimetric analysis (TGA) measurement was taken on a NETZSCH-TG-209F1 apparatus, and differential scanning calorimetry (DSC) experiments were performed on a DSC8500. Absorption spectra were taken on a Hitachi U-3010 UV-vis spectrophotometer. The film on quartz used for UV measurements was prepared by spin-coating with chloroform solution. The electrochemical cyclic voltammogram was obtained using a Zahner IM6e electrochemical workstation in a 0.1 mol/L tetrabutylammonium hexafluorophosphate (Bu_4NPF_6) acetonitrile solution. A Pt electrode coated with the sample film was used as the working electrode; a Pt wire and Ag/AgCl (0.01 M AgCl in acetonitrile) were used as the counter and reference electrodes, respectively.

OSCs were fabricated in the configuration of the traditional sandwich structure with an ITO positive electrode and a metal negative electrode. Patterned ITO glass with a sheet resistance of 30 Ω □-1 was purchased from CSG Holding Co., Ltd (China). The ITO glass was cleaned in an ultrasonic bath of acetone and isopropanol, and treated by UVO (ultraviolet ozone cleaner, Jelight Company, USA). Then a thin layer (30 nm) of PEDOT: PSS (poly(3,4-ethylenedioxythiophene)-poly(styrene sulfonate)) (Baytron PVP A1 4083, Germany) was spin-coated on the ITO glass. Then, the photoactive layer was prepared by spin-coating the blend solution of BDT-3T(3-Hex)-ID, BDT-3T(4-Hex)-ID and $PC_{71}BM$ (different weight ratio) on the top of the PEDOT:PSS layer and baked at 80°C for 0.5 h, respectively. The concentration of the solution was 10 mg/mL in chloroform. Finally, a metal electrode layer of Al was vacuum evaporated on the photoactive layer under a shadow mask in the vacuum of ca. 10^{-4} Pa. The current-voltage (I-V) measurement of the devices was conducted on a computer-controlled Keithley 236 Source Measure Unit. A xenon lamp coupled with A.M. 1.5 solar spectrum filters was used as light source, and the optical power at the sample was ca. 100 mW/cm^2.

Synthesis

Monomer 4 A mixture of monomer (1) (774.77 mg, 1 mmol), monomer (2) (1.152 g , 2.2 mmol), $Pd_2(dba)_3$ (14 mg), $[(CH_3)_3C]_3PHBF_4$ (18 mg), K_3PO_4 (20 ml, 2 M in aqueous solution) and toluene (30 ml), were stirred under the protection of N_2 flow. The solution was kept at 80 °C for 24 hrs. The mixture was poured into water, extracted with dichloromethane, and washed by water, dried over $MgSO_4$. After evaporation of the solvent, the residue was purified by column chromatography on silica gel (petroleum/CH_2Cl_2, 1:1) to produce 581.60 mg of red solid of product (4) with a yield of 41.3%. MALDI-TOF MS: 1407.7, calculated for $C_{80}H_{94}O_2S_{10}$ 1408.23. ^{1}H NMR (400 MHz, $CDCl_3$): δ ppm 9.82 (s, 2H), 7.62 (d, 4H), 7.31 (d, 2H), 7.25 (d, 2H), 7.13 (d, 4H), 6.96 (d, 2H), 2.98 (t, 4H), 2.85 (t, 4H), 2.78 (t, 4H), 1.84 (m, 4H), 1.72 (m, 8H), 1.53 (m, 4H), 1.41 (m, 14H), 1.34 (m, 18H), 0.95 (m, 18H).

Monomer 5 The synthesis procedure for monomer (5) is similar with that of monomer (4) but using precursor (3) instead of (2). After evaporation of the solvent, the residue was purified by column chromatography on silica gel (eluent petroleum/CH_2Cl_2, 2:1) to produce 736.5 mg of compound (5) with a yield of 52.3%. MALDI-TOF MS: 1407.9, calcd for $C_{80}H_{94}O_2S_{10}$ 1408.23. ^{1}H NMR ($CDCl_3$, 400 MHz): δ [ppm] 9.96 (d, 2H), 7.63 (s, 2H), 7.34 (d, 2H), 7.22(d, 2H), 7.07(d, 2H), 7.03 (d, 4H), 6.94 (d, 2H), 2.96 (m, 8H), 2.81 (t, 4H), 1.82 (m, 4H), 1.70 (m, 8H), 1.49 (t, 4H), 1.39 (m, 14H), 1.32 (m, 18H), 0.91(m, 18H).

BDT-3T(3-Hex)-ID To a solution of monomer (4) (200 mg, 0.14 mmol) in 30 mL of toluene, 1,3-indanedione (45.62 mg, 0.312 mmol) and 10 drops of piperidine were added and the mixture was refluxed at 90 °C for 12 hrs under nitrogen. After cooling to room temperature, the solution was adding chloroform and washed with water and dried over $MgSO_4$. After solvent removal, the residue was purified by column chromatography on silica gel (dichloromethane) to give 108.6 mg BDT-3T(3-Hex)-ID (yield: 45.9%) of black solid. MALDI-TOF MS: 1664.0, calculated for $C_{98}H_{102}O_4S_{10}$ 1664.49. ^{1}H NMR (400 MHz, $CDCl_3$): δ ppm 7.80 (s, 6H), 7.71 (m, 4H), 7.52 (s, 2H), 7.32 (s, 2H), 7.18 (s, 2H), 7.00-6.80 (m, 8H), 2.95 (t, 4H), 2.81 (t, 4H), 2.66 (t, 4H), 1.83 (m, 4H), 1.62 (m, 8H), 1.55 (m, 4H), 1.38 (m, 14H), 1.30 (m, 18H), 0.92 (m, 18H). Anal. Calcd for $C_{98}H_{102}O_4S_{10}$: C, 70.12; H, 6.188. Found: C, 69.02; H, 6.01.

BDT-3T(4-Hex)-ID To a solution of monomer (5) (200 mg, 0.14 mmol) in 30 mL of toluene, 1,3-indanedione (45.62 mg, 0.312

mmol) and 10 drops of piperidine were added. The mixture was refluxed at 110 °C for 12 hrs under nitrogen. After cooling to room temperature, the solution was adding chloroform and washed with water and dried over $MgSO_4$. After solvent removal, the residue was purified by column chromatography on silica gel (chloroform) to give 145.3 mg BDT-3T(4-Hex)-ID (yield: 61.5%) of black solid. MALDI-TOF MS: 1663.6, calculated for $C_{98}H_{102}O_4S_{10}$ 1664.49. ^{1}H NMR (400 MHz, $CDCl_3$): δ ppm 7.82 (m, 6H), 7.70 (m, 4H), 7.54 (d, 2H), 7.34 (d, 2H), 7.20 (d, 2H), 7.02-6.85 (m, 8H), 3.00 (t, 4H), 2.86 (t, 4H), 2.71 (t, 4H), 1.88 (m, 4H), 1.67 (m, 8H), 1.60 (m, 4H), 1.43 (m, 14H), 1.35 (m, 18H), 0.97 (m, 18H). Anal. Calcd for $C_{98}H_{102}O_4S_{10}$: C, 70.72; H, 6.18. Found: C, 69.92; H, 6.08.

Results and discussion

Synthesis

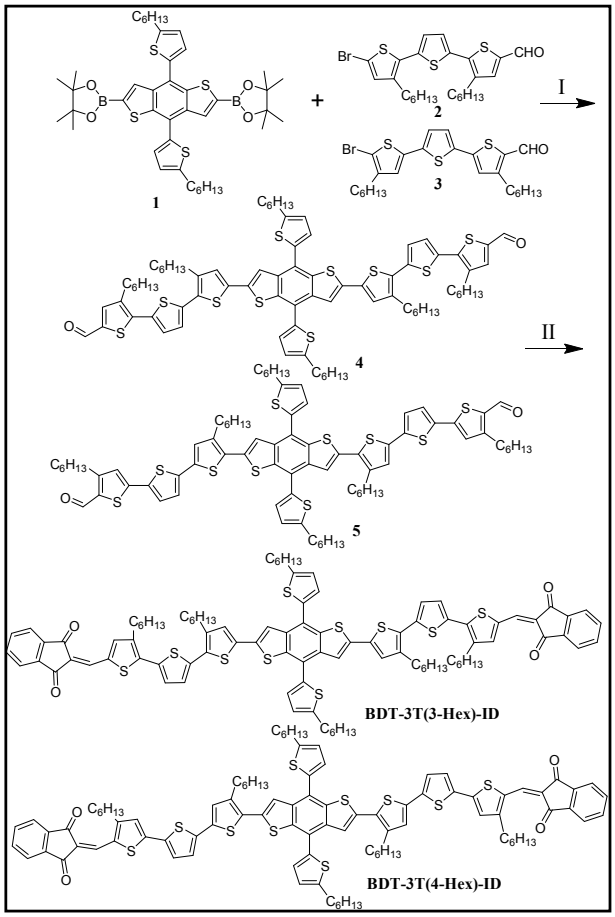

Scheme 1 Structure and synthetic routes of BDT-3T(3-Hex)-ID and BDT-3T(4-Hex)-ID: I) $Pd_2(dba)_3$, $[(CH_3)_3C]_3PHBF_4$, K_3PO_4 (2 mol/L), toluene, 80 °C for 24 hrs; II) 1,3-indanedione, toluene, under N_2, 90 °C or 110 °C for 12 hrs.

In Scheme 1, it is shown the structures and the synthetic routes for the new compounds of BDT-3T(3-Hex)-ID and BDT-3T(4-Hex)-ID. Monomer 1, 2 and 3 were obtained according to literatures.[45-47] Compound 4 and 5 were synthesized from monomer 1, 2 and 3 through Suzuki reaction with a yield of 41.3% and 52.3%, respectively. Finally, BDT-3T(3-Hex)-ID and BDT-3T(4-Hex)-ID were prepared by Knoevenagel condensation of 1,3-indenedione with the corresponding aldehyde derivatives. Both BDT-3T(3-Hex)-ID and BDT-3T(4-Hex)-ID are soluble in common organic solvents, such as chloroform, tetrahydronfuran and toluene. But BDT-3T(4-Hex)-ID shows better solubility compared with BDT-3T(3-Hex)-ID.

Thermal stability

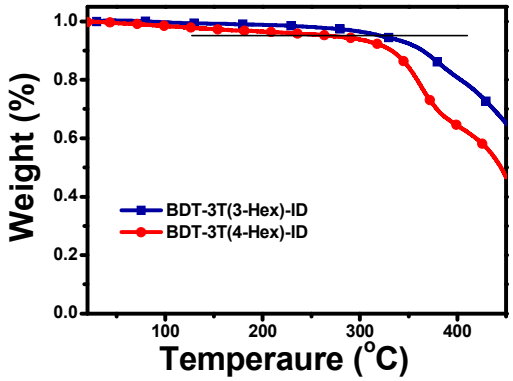

Fig 1 TGA plot for BDT-3T(3-Hex)-ID and BDT-3T(4-Hex)-ID.

To make sure BDT-3T(3-Hex)-ID and BDT-3T(4-Hex)-ID are stable enough for the applications in photovoltaic solar cells, the TGA investigations were taken under nitrogen. As shown in Figure 1, the temperatures with 5% weight loss for BDT-3T(3-Hex)-ID and BDT-3T(4-Hex)-ID are at 320 °C and 270 °C, respectively, which indicate that these two compounds are stable for device application. Both of BDT-3T(3-Hex)-ID and BDT-3T(4-Hex)-ID exhibit no apparent DSC peaks (ESI Figure S1), which demonstrate the materials do not show any crystallization behavior.

Optical properties

The UV-vis absorption spectra of BDT-3T(3-Hex)-ID and BDT-3T(4-Hex)-ID in solutions and solid films are shown in Figure 2. The absorption spectrum of BDT-3T(3-Hex)-ID solution shows two absorption peaks at 420 and 536 nm, respectively, covering a broad wavelength range from 350 nm to 650 nm, which is benefited from A-D-A molecular structure. The maximum visible absorption peak is attributed to the intramolecular charge transfer transition between the BDT unit and ID unit. The absorption spectrum of BDT-3T(4-Hex)-ID solution shows the similar properties. The molar absorbance is $1.01*10^5$ for BDT-3T(3-Hex)-ID and $1.16*10^5$ for BDT-3T(4-Hex)-ID, respectively, which are among the high molar absorbance of the photovoltaic materials. The absorption spectra of the BDT-3T(3-Hex)-ID and BDT-3T(4-Hex)-ID films are covering a broad wavelength range from 400 nm to 750 nm and both red shifted comparing with the solution absorbance, which result from the aggregation of the molecules in the film state. The absorption edge of BDT-3T(3-Hex)-ID and BDT-3T(4-Hex)-ID films are at ca. 790 nm and ca. 750 nm, corresponding to the band gap of 1.53 eV and 1.61 eV, respectively. The detailed optical data of BDT-3T(3-Hex)-ID and

BDT-3T(4-Hex)-ID are listed in Table 1. Compared with BDT-3T(3-Hex)-ID, the absorption peak of BDT-3T(4-Hex)-ID are red-shifted by ca. 20 nm in solution, the absorption edge of BDT-3T(4-Hex)-ID is blue-shifted by ca. 40 nm in film, and the molar absorbance of BDT-3T(4-Hex)-ID is a little higher, owing to the different substitute position of the side alkyl chains in the molecular structure. These results indicate that the alkyl side chains concentrated in the center part of the terthiophene backbone (BDT-3T(3-Hex)-ID) is benefit for the aggregation of the molecules in the film state, and for BDT-3T(4-Hex)-ID, the chains distributed in the peripheral part of the terthiophene backbone (BDT-3T(4-Hex)-ID) is good for the intramolecular charge transfer transition.

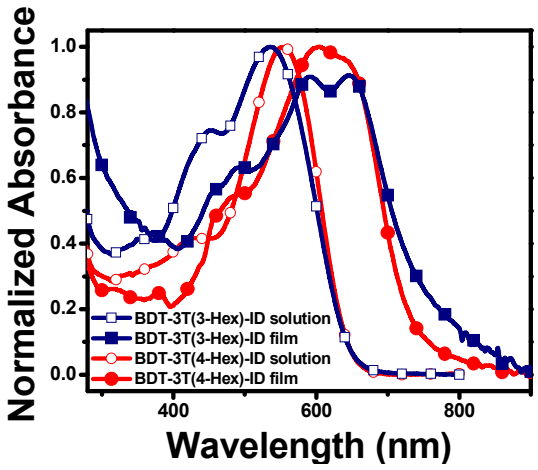

Fig 2 UV-vis absorption spectra of BDT-3T(3-Hex)-ID and BDT-3T(4-Hex)-ID in chloroform solution and in film state.

Table 1. Optical properties and electrochemical properties for BDT-3T(3-Hex)-ID and BDT-3T(4-Hex)-ID.

Compounds	$\lambda_{solution}$ (nm)	λ_{film} (nm)	ε (L.mol^{-1}.cm^{-1})	$(E_g^{opt})_{film}$ (eV)	E^{red}_{onset} (V vs Ag/AgCl)	E_{LUMO} (eV)	E^{ox}_{onset} (V vs Ag/AgCl)	E_{HOMO} (eV)
BDT-3T(3-Hex)-ID	536	594	1.01*10^5	1.53	-0.67	-3.73	0.95	-5.35
BDT-3T(4-Hex)-ID	554	606	1.16*10^5	1.61	-0.78	-3.62	0.85	-5.25

HOMO and LUMO energy levels

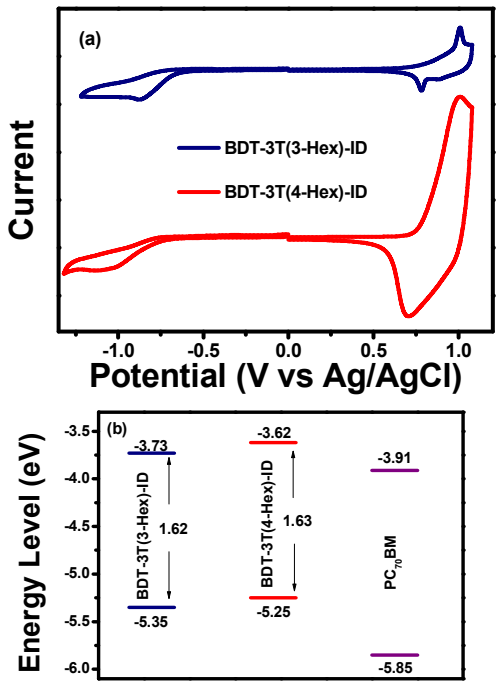

Fig 3 (a)Cyclic voltammogram of BDT-3T(3-Hex)-ID and BDT-3T(4-Hex)-ID film on Pt electrode in an acetonitrile solution of 0.1 mol/L Bu_4NPF_6 with a scan rate of 100 mV/s. (b) Energy levels of BDT-3T(3-Hex)-ID and BDT-3T(4-Hex)-ID.

Electrochemical cyclic voltammetry of BDT-3T(3-Hex)-ID and BDT-3T(4-Hex)-ID films on Pt electrode was carried out which is shown in Figure 3 (a). The onset oxidation and reduction potentials (E^{ox}_{onset}, E^{red}_{onset}) of BDT-3T(3-Hex)-ID were measured to be 0.95 and -0.67 V vs Ag/AgCl. The HOMO energy level (E_{HOMO}), the LUMO energy levels (E_{LUMO}) and the electrochemical band gap (E_g) of BDT-3T(3-Hex)-ID were calculate to be -5.35, -3.73 and 1.62 eV, respectively, according to the following equations:[48] E_{HOMO} = -e (E^{ox}_{onset} + 4.40) (eV), E_{LUMO} = -e (E^{red}_{onset} + 4.40) (eV) and Eg = E_{LUMO} - E_{HOMO}. For BDT-3T(4-Hex)-ID, the E^{ox}_{onset} and E^{red}_{onset} were measured to be 0.85 and -0.75 V vs Ag/AgCl. Thus E_{HOMO}, E_{LUMO} and E_g of BDT-3T(4-Hex)-ID were estimated to be -5.25, -3.62 and 1.63 eV, respectively. The electrochemical band gaps of BDT-3T(3-Hex)-ID and BDT-3T(4-Hex)-ID are coincident with the optical measurements in reasonable margin of error. Compared with the HOMO and LUMO energy levels of $PC_{71}BM$,[49] the two compounds are appropriate to be used as the photovoltaic donor materials. From the energy levels of BDT-3T(3-Hex)-ID and BDT-3T(4-Hex)-ID (Figure 3 (b)), it can be seen that the different substitute position of the side alkyl chains also affects the electrochemical properties of the compounds. The results indicate that inboard configuration of the alkyl side chains in BDT-3T(3-Hex)-ID is profitable for lowering the HOMO energy level, which may lead a higher V_{oc}. However in photovoltaic device, its lower HOMO energy didn't result in an expected larger V_{oc}. Probably, the rougher film morphology of the photoactive layer, hole mobility of the material, or higher energy loss,[26] etc. influenced the V_{oc}. The E^{ox}_{onset}, E^{red}_{onset},

E_{LUMO} and E_{HOMO} values of the compounds are also listed in Table 1.

Photovoltaic properties of OSCs

Bulk-heterojunction OSCs with ITO/PEDOT: PSS/ photoactive layer /Al structure were fabricated by using BDT-3T(3-Hex)-ID or BDT-3T(4-Hex)-ID as donor materials, $PC_{71}BM$ as acceptors[50-52] with donor/acceptor weight ratio (1.5:1, w/w), and Al as the negative electrode. The typical current-voltage curves of the OSCs at dark and under the illumination of AM 1.5, 100 mW/cm^2 are shown in Figure 4. The photovoltaic performance data of the OSCs are summarized in Table 2. The OSC device based on BDT-3T(4-Hex)-ID demonstrated a V_{oc} of 0.87 V, a J_{sc} of 8.82 mA/cm^2, a *FF* of 68.9%, corresponding to a PCE of 5.30%, under the illumination of AM 1.5, 100 mW/cm^2. At the same time, the photovoltaic performance of the OSC based on BDT-3T(3-Hex)-ID showed a V_{oc} of 0.75 V, a J_{sc} of 4.0 mA/cm^2, a *FF* of 35.3%, corresponding to a PCE of 1.06%, under the same experimental conditions. Obviously, the peripherally distributed side chains in BDT-3T(4-Hex)-ID) plays an important role for the much better photovoltaic performance. To optimize the OSCs device by changing the donor/acceptor weight ratio from 1.5:1 to 1.25:1, the device based on BDT-3T(3-Hex)-ID shows similar result, but the device based on BDT-3T(4-Hex)-ID shows a better result that a V_{oc} of 0.87 V, a J_{sc} of 10.54 mA/cm^2, a *FF* of 71.4%, corresponding to a PCE of 6.55%, under the illumination of AM 1.5, 100 mW/cm^2.

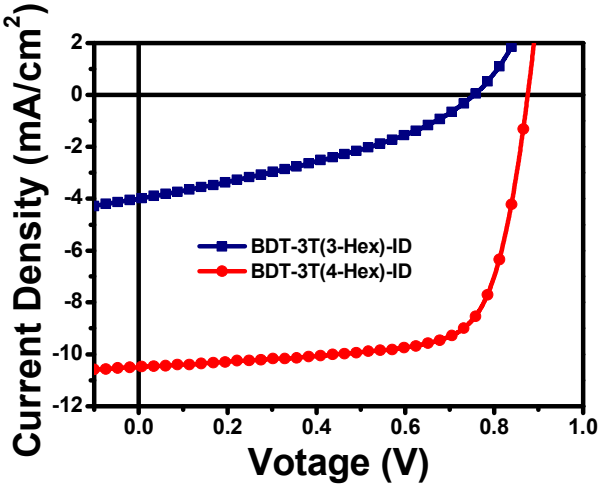

Fig 4 Current density-voltage characteristics of the OSC devices based on the blend of molecular material/$PC_{71}BM$ with Al as the negative electrode at dark and under the illumination of AM 1.5, 100 mW/cm^2.

Table 2 Photovoltaic properties of ITO/PEDOT: PSS/Active layer/Al under the illumination of AM 1.5, 100 mW/cm^2.

Composition of active layer	V_{oc} (V)	J_{sc} (mA/cm^2)	*FF* (%)	PCE (%)
BDT-3T(3-Hex)-ID:$PC_{71}BM$ (1.5:1, w/w)	0.75	4.0	35.3	1.06
BDT-3T(4-Hex)-ID:$PC_{71}BM$ (1.5:1, w/w)	0.87	8.82	68.9	5.30
BDT-3T(4-Hex)-ID:$PC_{71}BM$ (1.25:1, w/w)	0.87	10.54	71.4	6.55

Morphology

To investigate the evidence of the big difference in photovoltaic properties between BDT-3T(3-Hex)-ID and BDT-3T(4-Hex)-ID, we utilize atomic force microscope (AFM) to investigate the morphology of blend films composing by the molecular material and $PC_{71}BM$ (the weight ratio is the same with the best device). For the photovoltaic performance of OSCs, the morphology of the photoactive layer is very significant. [53-54] All of the AFM images of the blend films are showed in Figure 5. Both of the films exhibit typical amorphous morphology without any crystalline domains. We can see intuitively that the surface of the blend film of BDT-3T(4-Hex)-ID/$PC_{71}BM$ is more neat, which will be beneficial for the charge separation and charge transport in the OSC devices. However, the blend film of BDT-3T(3-Hex)-ID/$PC_{71}BM$ exhibit rougher morphology and big aggregates, which could influence the charge separation and the charge transport negatively.

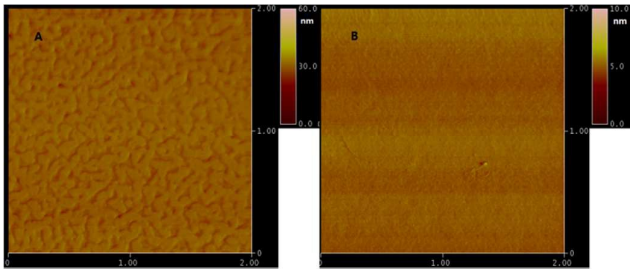

Fig 5 Atomic Force Microscope images of molecules: $PC_{71}BM$ films spin-coated from the blend solutions: (a) BDT-3T(3-Hex)-ID/$PC_{71}BM$ (1.5:1, w/w), (b) BDT-3T(4-Hex)-ID/$PC_{71}BM$ (1.25:1, w/w). The scan size for all images is 2μm×2μm.

Conclusions

Two new A-D-A molecules with bithienyl-substituted benzodithiophene (BDT) as core and donor unit, indenedione (ID) as end group and acceptor unit, 3,3''-dihexyl-2,2':5',2''-terthiophene (3T(3-Hex)) or 4,4''-dihexyl-2,2':5',2''-

terthiophene (3T(4-Hex)) as π bridge, BDT-3T(3-Hex)-ID and BDT-3T(4-Hex)-ID, were designed and synthesized. Compared with BDT-3T(3-Hex)-ID, the absorption peak of the BDT-3T(4-Hex)-ID is red shifted by ca. 20 nm in solution, the molar absorbance is higher and the AFM image shows better morphology, benefitted from the outward alkyl side chain. All these super properties contribute to the outstanding PCE of the OSC based on the blend of BDT-3T(4-Hex)-ID and $PC_{71}BM$ (1.25:1, w/w), reaching 6.55% with a J_{sc} of 10.54 mA/cm^2 and a V_{oc} of 0.87 V, under the illumination of AM.1.5, 100 mW/cm^2. While the PCE of the OSC based on BDT-3T(3-Hex)-ID as donor material is 1.06% under the similar experimental conditions. There is just a tiny change in the substituent position of the side alkyl chains in the molecular structure for BDT-3T(3-Hex)-ID and BDT-3T(4-Hex)-ID. But the BDT-3T(3-Hex)-ID and BDT-3T(4-Hex)-ID shows a great difference in the absorption properties, the HOMO and LUMO energy level, especially the performance of the OSCs device and the AFM images. The alkyl side chains distributing in the peripheral of the π bridge backbone to form outward configuration is a profitable strategy in the molecular structure to get a competitive OSCs performance in the BDT-ID system. This work riches the example contributing to a better understanding of the structure-property relation in organic photovoltaic materials.

Acknowledgements

This work was supported by the China Postdoctoral Science Foundation (2013M530574), the National Natural Science Foundation of China (51272033, 51572037), the Priority Academic Program Development of Jiangsu Higher Education Institutions.

Notes and references

1 J. Cremer, P. Bauerle, *J. Mater. Chem.*, 2006, **16**, 874-884.
2 Y. Shirota, H. Kageyama, *Chem. Rev.*, 2007, **107**, 953-1010.
3 M. L. Sun, L. Wang, X. H. Zhu, B. Du, R. Liu, W. Yang, Y. Cao, et al., *Solar Energy Materials and Solar Cells*, 2007, **137**, 1681-1687.
4 C. Q. Ma, E. Mena-Osteritz, T. Debaerdemaeker, M. M. Wienk, R. A. J. Janssen, P. Bauerle, Angew. *Chem. Int. Ed.,* 2007, **46**, 1679-1683.
5 S. Roquet, A. Cravino, P. Leriche, O. Aleveque, P. Frere, J. Roncali, *J. Am. Chem. Soc.,* 2006, 128, 3459-3466.
6 J. Roncali, *Acc. Chem. Res.*, 2009, **42**, 1719-1730.
7 J. Zhang, Y. Yang, C. He, Y. J. He, G. J. Zhao, Y. F. Li, *Macromolecules*, 2009, **42**, 7619-7622.
8 H. X. Shang, H. J. Fan, Y. Liu, W. P. Hu, Y. F. Li, X. W. Zhan, *Adv. Mater.*, 2011, **23**, 1554-1557.
9 J. Min, Y. N. Luponosov, A. Gerl, S. Grigorian, *Adv. Energy. Mater.*, 2014, **4**.
10 C. He, Q. G. He, Y. P. Yi, G. L. Wu, F. L. Bai, Z. G. Shuai, Y. F. Li, et al., *J. Mater. Chem.*, 2008, **18**, 4085-4090.
11 A. B. Tamayo, B. Walker, T. Q. Nguyen, *J. Phys. Chem. C*, 2008, **112**, 11545-11551.
12 B. Walker, A. B. Tomayo, X. D. Dang, P. Zalar, J. H. Seo, A. Garcia, M. Tantiwiwat, T. Q. Nguyen, *Adv. Funct. Mater.*, 2009, **119**, 3063-3069.
13 S. L. Shen, J. Pei, C. He, J. Zhang, P. Shen, Y. Zhang, Y. P. Yi, Z. J. Zhang, Z. B. Li, Y. F. Li, *Chem. Mater.*, 2013, **25**, 2274-2281.
14 C. H. Cui, X. Guo, J. Min, B. Guo, X. Cheng, M. J. Zhang, C. J. Brabec, Y. F. Li, *Adv. Mater.*, 2015, 27, 7469-7475.
15 Y. M. Sun, G. C. Welch, W. L. Leong, C. J. Takacs, G. C. Bazan, A. J. Heeger, *Nat. Mater.*, 2012, 11, 44-48.
16 Z. B. Henson, G. C. Welch, T. van der Poll, G. C. Bazan, *J. Am. Chem. Soc.*, 2012, **134**, 3766-3779.
17 D. Deng, Y. J. Zhang, L. Yuan, C. He, K. Lu, Z. X. Wei, *Adv. Energy. Mater.*, 2014, **4**, 1400538.
18 L. Yuan, Y. F. Zhao, J. Q. Zhang, Y. J. Zhang, L. Y. Zhu, K. Lu, W. Yan, Z. X. Wei, *Adv. Mater.*, 2015, **27**, 4229-4233.
19 X. W. Zhu, B. Z. Xia, K. Lu, H. Li, R. M. Zhou, Y. J. Zhang, Z. G. Shuai, Z. X. Wei, *Chem. Mater.*, 2016, **28**, 943-950.
20 J. Y. Zhou, X. J. Wan, Y. S. Liu, Y. Zuo, Z. Li, G. R. He, G. K. Long, W. Ni, C. X. Li, X. C. Su, Y. S. Chen, *J. Am. Chem. Soc.*, 2012, **134**, 16345-16351.
21 B. Kan, M. Li, Q. Zhang, F. Liu, X. Wan, Y. Wang, W. Ni, G. Long, X. Yang, H. Feng, Y. S. Chen, *J. Am. Chem. Soc.*, 2015, **137**, 3886-3893.
22 D. Sun, D. Meng, Y. H. Cai, B. B. Fan, Y. Li, W. Jiang, L. J. Huo, Y. M. Sun, Z. H. Wang, *J. Am. Chem. Soc.*, 2015, **137**, 11156-11162.
23 Y. Z. Lin, Q. He, F. W. Zhao, L. J. Huo, J. Q. Mai, X. H. Lu, C. J. Su, T. F. Li, J. Y. Wang, J. S. Zhu, Y. M. Sun, C. R. Wang, X. W. Zhan, *J. Am. Chem. Soc.*, 2016, 138, 2973-2976.
24 Y. Z. Lin, J. Wang, Z.-G. Zhang, H. Bai, Y. F. Li, D. B. Zhu, X. W. Zhan, Adv. Mater., 2015, **27**, 1170-1174.
25 H. J. Bin, Z. -G. Zhang, L. Gao, S. S. Chen, L. Zhong, L. W. Xue, C. Yang, Y. F. Li, *J. Am. Chem. Soc.*, 2016, 138, 4657-4664.
26 K. Gao, L. S. Li, T. Q. Lai, L. G. Xiao, Y. Huang, F. Huang, J. B. Peng, Y. Cao, F, Liu, T. P. Russell, R. A. J. Janssen, X. B. Peng, *J. Am. Chem. Soc.*, 2015, **137**, 7282-7285.
27 Z.-G. Zhang, Y. F. Li, *Sci. China Chem.*, 2015, **58**, 192-209.
28 H. Sirringhaus, P. J. Brown, R. H. Friend, M. M. Nielsen, K. Bechgaard, B. M. W. Langeveld-Voss, A. J. H. Spiering, R. A. J. Janssen, E. W. Meijer, P. Herwig, D. M. de Leeuw, *Nature*, 1999, **401**, 685-688.
29 H. J. Chen, Y. L. Guo, G. Yu, Y. Zhao, J. Zhang, D. Gao, H. T. Liu, Y. Q. Liu, *Adv. Mater.*, 2012, **24**, 4618-4622.
30 R. Boese, H.-C. Weiss, D. Bläser, *Angew. Chem. Int. Ed.*, 1999, **38**, 988-992.
31 S. Saito, K. Nakakura, S. Yamaguchi, *Angew. Chem. Int. Ed.*, 2012, **51**, 714-717.
32 L. Biniek, S. Fall, C. L. Chochos, D. V. Anokhin, D. A. Ivanov, N. Leclerc, P. Lévêque, T. Heiser, *Macromolecules*, 2010, **43**, 9779-9786.
33 S. Ko, E. T. Hoke, L. Pandey, S. Hong, R. Mondal, C. Risko, Y. P. Yi, R. Noriega, M. D. McGehee, J.-L. Brédas, A. Salleo, Z. N. Bao, *J. Am. Chem. Soc.*, 2012, **134**, 5222-5232.
34 Q. H. Wu, M. Wang, X. L. Qiao, Y. Xiong, Y. G. Huang, X. K. Gao, H. X. Li, *Macromolecules*, 2013, **46**, 3887-3894.
35 C. Cabanetos, A. El Labban, J. A. Bartelt, J. D. Douglas, W. R. Mateker, J. M. J. Fréchet, M. D. McGehee, P. M. Beaujuge, *J. Am. Chem. Soc.*, 2013, **135**, 4656-4659.
36 V. S. Gevaerts, E. M. Herzig, M. Kirkus, K. H. Hendriks, M. M. Wienk, J. Perlich, P. Muller-Buschbaum, R. A. J. Janssen, *Chem. Mater.*, 2014, **26**, 916-926.
37 T. Lei, J. Y. Wang, J. Pei, *Chem. Mater.*, 2014, **26**, 594-603.
38 C. H. Cui, J. Min, C. -L. Ho, T. Ameri, P. Yang, J. Z. Zhao, C. J. Brabec, W. -Y. Wong, *Chem. Commun.*, 2013, **49**, 4409-4411.
39 C. H. Cui, W. -Y. Wong, Y. F. Li, *Energy Environ. Sci.*, 2014, **7**, 2276-2284.
40 X. L. Liu, S. S. Li, J. H. Li, J. Wang, Z. Tan, F. Yan, H. Li, Y. H. Lo, C. -H. Chui, W. -Y. Wong, RSC Adv., 2014, **4**, 63260-63267.
41 S. Chen, L. G. Xiao, X. J. Zhu, X. B. Peng, W. -K. Wong, W. -Y. Wong, *Chem. Commun.*, 2015, **51**, 14439-14442.
42 C. H. Cui, W. -Y. Wong, *Macromol. Rapid Commun.*, 2016, **37**, 287-302.

43 C. H. Cui, Z. C. He, Y. Wu, X. Cheng, H. B. Wu, Y. F. Li, Y. Cao, W.-Y. Wong, *Energy Environ. Sci.*, 2016, **9**, 885-891.
44 H. D. Wang, L. G. Xiao, L. Yan, S. Chen, X. J. Zhu, X. B. Peng, X. Z. Wang, W. -K. Wong, W. -Y. Wong, *Chem. Sci.*, 2016, DOI: 10.1039/c5sc04783h.
45 S. Tanaka, G. Tatsuta, A. Sugie, A. Mori, *Tetrahedron Letter*, 2013, **54**, 1976-1979.
46 J. Cheng, X. Z. Liang, Y. X. Cao, K. P. Guo, W. Y. Wong, *Tetrahedron*, 2015, **71**, 5634-5639.
47 R. K. Chen, X. C. Yang, H. N. Tian, X. N. Wang, A. Hagfeldt, L. C. Sun, *Chem. Mater.*, 2007, **19**, 4007-4015.
48 Y. F. Li, Y. Cao, J. Gao, D. L. Wang, G. Yu, A. J. Heeger, *Synth. Met.*, 1999, **99**, 243-248.
49 Y. J. He, G. J. Zhao, B. Peng, Y. F. Li, *Adv. Funct. Mater.*, 2010, **20**, 3383-3389.
50 M. M. Wienk, J. M. Kroon, W. J. H. Verhees, J. Knol, J. C. Hummelen, P. A. van Hal, R. A. J. Janssen, *Angew. Chem. Int. Ed.*, 2003, **42**, 3371-3375.
51 F. B. Kooistra, V. D. Mihailetchi, L. M. Popescu, D. Kronholm, P. W. M. Blom, J. C. Hummelen, *Chem. Mater.*, 2006, **18**, 3068-3073.
52 B. C. Thompson, J. M. J. Frechet, *Angew. Chem. Int. Ed.*, 2008, **47**, 58-77.
53 W. L. Ma, C. Y. Yang, X. Gong, K. Lee, A. J. Heeger, *Adv. Funct. Mater.*, 2015, **15**, 1617-1622.
54 G. Li, V. Shrotriya, J. S. Huang, Y. Yao, T. Moriarty, K. Emery, Y. Yang, *Nature Materials*, 2005, **4**, 864-868.

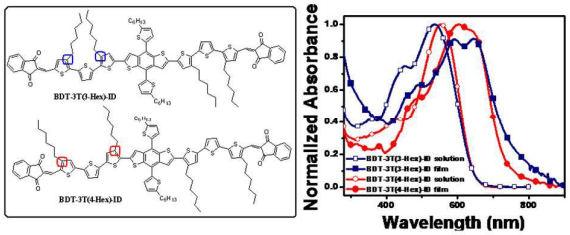

Two new compounds with the alkyl side chains at different position own the similar structure, but exhibit different photovoltaic properties.